Ca^{2+}-independent activation of BK_{Ca} channels at negative potentials in mammalian inner hair cells

Henrike Thurm, Bernd Fakler and Dominik Oliver

Department of Physiology, University of Freiburg, Hermann-Herder-Strasse 7, 79104 Freiburg, Germany

The defining characteristic of large-conductance Ca^{2+}- and voltage-activated K^+ channels (BK_{Ca}) is their allosteric activation by two distinct stimuli, membrane depolarization and cytosolic Ca^{2+} ions. In this allosteric gating, increasing cytosolic Ca^{2+} concentration ($[Ca^{2+}]_i$) shifts the depolarization required for channel opening into the physiological voltage range. In fact, according to present knowledge, elevation of $[Ca^{2+}]_i$ to micromolar levels is the only means to activate BK_{Ca} at membrane potentials below 0 mV. We recorded BK_{Ca}-mediated currents from auditory inner hair cells (IHCs) in acutely isolated organs of Corti using the patch-clamp technique in whole-cell and excised patch configuration. In inside-out and outside-out patches, activation of BK_{Ca} channels from IHCs showed the prototypic sensitivity to increased $[Ca^{2+}]_i$. However, channel activation at 0 $[Ca^{2+}]_i$ occurred at unusually negative potentials (half-maximal activation (V_h) around 0 mV), indicating that a large fraction of the channels can be activated at physiological voltages without elevated $[Ca^{2+}]_i$. In intact IHCs, the activation curve of BK_{Ca} currents recorded in whole-cell configuration exhibited a V_h of −42 mV together with a high voltage dependence (slope factor of 10 mV) and submillisecond onset of current. Surprisingly, this activation was independent of changes in local $[Ca^{2+}]_i$ as shown by experiments that interfered with Ca^{2+} influx through voltage-gated Ca^{2+} (Cav) channels, release of Ca^{2+} from internal stores, or intracellular buffer capacity. This behaviour is not due to β-subunits of BK_{Ca} ($BK\beta$), as genetic inactivation of the β-subunit expressed in IHCs, KCNMB1, did not affect BK_{Ca} gating. We conclude that the BK_{Ca} channel protein in IHCs may be modified in order to rapidly activate and deactivate at resting $[Ca^{2+}]_i$. Our results suggest that BK_{Ca} may function as a purely voltage-gated K^+ channel with exceptionally rapid activation kinetics, challenging the view that both increased cytosolic Ca^{2+} and depolarization are generally required for activation of BK_{Ca}.

(Resubmitted 14 July 2005; accepted after revision 2 September 2005; first published online 8 September 2005)
Corresponding author D. Oliver: Physiologisches Institut, Universität Freiburg, Hermann-Herder-Strasse 7, 79104 Freiburg, Germany. Email: dominik.oliver@physiologie.uni-freiburg.de

BK_{Ca} channels are key modulators of cellular excitability (Vergara *et al.* 1998). They are assembled from four identical α-subunits of BK_{Ca} ($BK\alpha$) encoded by the *Slo* gene (Adelman *et al.* 1992) and are dually activated by membrane depolarization and increase in intracellular Ca^{2+} concentration ($[Ca^{2+}]_i$) (Marty, 1981; Pallotta *et al.* 1981; Latorre *et al.* 1982). Increasing $[Ca^{2+}]_i$ shifts the voltage required for channel activation in the hyperpolarizing direction (Cui *et al.* 1997; Horrigan & Aldrich, 2002). The precise voltage range of activation and the calcium sensitivity may be affected by different mechanisms including alternative mRNA splicing of $BK\alpha$ (Adelman *et al.* 1992; Tseng-Crank *et al.* 1994), coassembly with β-subunits (KCNMB1–4; McManus *et al.* 1995; Brenner *et al.* 2000*a*) or accessory proteins (Schopperle *et al.* 1998; Xia *et al.* 1998), and post-translational modification (Reinhart *et al.* 1991; DiChiara & Reinhart, 1997; Schubert & Nelson, 2001). However, the exact impact of the latter on both voltage-dependence and Ca^{2+} sensitivity has often not been determined rigorously. Despite this variability, the activation range at resting $[Ca^{2+}]_i$ is generally not within the physiological voltage range (see Fig. 1*E*; e.g. Tseng-Crank *et al.* 1994; Brenner *et al.* 2000*a*; Ransom *et al.* 2003). Thus, it is assumed that under physiological conditions, BK_{Ca} channel opening inevitably requires coincident increase in $[Ca^{2+}]_i$ and membrane depolarization (Vergara *et al.* 1998).

In essentially all vertebrate auditory hair cells, BK_{Ca} carries a major component of the ionic current. In non-mammalian hair cells, activation of BK_{Ca} close to

 DOI: 10.1113/jphysiol.2005.094680

the resting potential results from Ca^{2+} entry through voltage-gated Ca^{2+} channels (Cav). Both channel types generally appear to be tightly colocalized allowing for a local activation route of BK_{Ca} channels by Cav (Roberts *et al.* 1990; Samaranayake *et al.* 2004). Consequently, blocking the Ca^{2+} current leads to a reduction of BK_{Ca} channel activity (Hudspeth & Lewis, 1988*a*; Art *et al.* 1993). In amphibian, reptilian and avian IHCs, the functional coupling between Cav-mediated Ca^{2+} influx and BK_{Ca}-mediated outward currents generates resonant behaviour of the membrane potential that contributes to the tuning of hair cells to specific sound frequencies (Art & Fettiplace, 1987; Fuchs *et al.* 1988; Hudspeth & Lewis, 1988*b*).

In contrast, mammalian IHCs do not exhibit significant electrical resonance. Yet, they exhibit a rapidly activating K^+ current (termed $I_{K,f}$ for its fast activation kinetics; Kros & Crawford, 1990) thought to be mediated by BK_{Ca} channels based on its Ca^{2+}-dependent gating observed in excised patches (Oliver *et al.* 2003) and its sensitivity to iberiotoxin, charybdotoxin and TEA (Kros *et al.* 1998; Marcotti *et al.* 2004; Pyott *et al.* 2004; Hafidi *et al.* 2005). In intact IHCs, this current exhibits a voltage range of activation similar to that of the L-type Cav channel of the hair cell (Cav1.3; Platzer *et al.* 2000). However, it has been a puzzle since its first description that $I_{K,f}$ was unaffected by removal of extracellular Ca^{2+} (Kros & Crawford, 1990; Marcotti *et al.* 2004). This apparent paradox may be explained by another voltage-dependent Ca^{2+} source providing increased $[Ca^{2+}]_i$ such as release from intracellular stores (Marcotti *et al.* 2004). To elucidate the mechanism that underlies the unusual BK_{Ca} gating in IHCs, we performed patch-clamp recordings in excised patches at defined $[Ca^{2+}]_i$ and in whole-cell configuration while interfering with $[Ca^{2+}]_i$. Surprisingly BK_{Ca} channels of IHCs could be activated at negative membrane potentials of around −40 mV without any increase in $[Ca^{2+}]_i$. Activation at negative potentials was observed both in excised patches and in whole-cell conditions, pointing towards a direct modification of the channel protein.

Methods

Tissue preparation

Apical cochlear turns of rats and mice (19–28 days after birth) were prepared as previously described (Oliver *et al.* 2000). Briefly, animals were anaesthetized with isoflurane, killed by decapitation, and the cochleae were dissected. After removal of the cochlear bone, the apical cochlear turn was separated from the modiolus. Stria vascularis and tectorial membrane were stripped off. This whole-mount preparation was placed into an experimental chamber continuously perfused with standard extracellular solution containing (mM): NaCl 144, KCl 5.8, $CaCl_2$ 1.3, $MgCl_2$ 0.9, Hepes 10, Na_2HPO_4 0.7 and glucose 5.6; pH adjusted to 7.4 with NaOH.

Most experiments were performed with IHCs from Wistar rats (Charles River Laboratories, Sulzfeld, Germany). BKα−/− mice were kindly provided by Dr P. Ruth (Department of Pharmacology and Toxicology, Tübingen, Germany; Sausbier *et al.* 2004). Experiments were performed on homozygous BKα−/− and BKα+/+129svj inbred littermates (Ruttiger *et al.* 2004). BKβ1−/− mice had a mixed 129svj/C57BL background (Brenner *et al.* 2000*b*) and were kindly provided by Dr M. Knipper (Hearing Research Center, Tübingen, Germany). 129svj inbred mice were used as a control. All animal use was performed according to institutional guidelines at the University of Freiburg.

Electrophysiological recordings

Voltage-clamp recordings were performed with an Axopatch 200B amplifier (Axon Instruments, Union City, CA, USA) at room temperature (20–24°C). Current recordings were low-pass filtered at 10 kHz and sampled at 25–100 kHz. Electrodes were pulled from quartz glass, were coated with Sylgard for excised patch experiments, and had initial resistances of 1.2–2.5 MΩ. During whole cell measurements, series resistance was typically 2–5 MΩ. Careful series resistance compensation (90–95%) was applied during all whole-cell experiments and voltages were corrected offline for errors due to residual series resistance.

Extracellular solutions were exchanged via a thin glass capillary (diameter, ∼100 μm) placed close to the IHCs. Either standard solution or one of the following modified extracellular solutions was applied. (i) For removal of all extracellular Ca^{2+}, Ca^{2+} was replaced by 1.3 mM Mg^{2+}, and 5 mM BAPTA was added. (ii) For external solution containing Sr^{2+}, Ca^{2+} was replaced by 1.3 mM Sr^{2+}. (iii) To measure currents through Cav channels, 35 mM Na^+ was replaced by an equal concentration of TEA^+. (iv) Complete removal of Na^+ was achieved by replacement with an equal concentration of *N*-methyl-D-glucamine ($NMDG^+$). Extracellular solutions usually contained 1 μM XE991 to block KCNQ-mediated potassium currents ($I_{K,n}$; Oliver *et al.* 2003).

For most whole-cell measurements, pipettes were filled with a KCl-based intracellular solution containing (mM): KCl 135, $MgCl_2$ 3.5, EGTA 5, Hepes 5, Na_2ATP 2.5 and 4-aminopyridine (4-AP) 10; pH adjusted to 7.3 with HCl. For one set of experiments, EGTA was replaced by either 0.1 or 30 mM BAPTA (either from Fluka, Seelze, Germany or Molecular Probes, Eugene, OR, USA). An appropriate amount of KCl was added to keep the osmolarity (285 mosmol l^{-1}) constant. The effective

concentration of BAPTA in these solutions was verified by titration using a Ca^{2+}-sensitive electrode (World Precision Instruments, Berlin, Germany). Measurement of $[Ca^{2+}]$ in the absence of any Ca^{2+} buffer revealed a contamination with 3 μM Ca^{2+}. Thus free $[Ca^{2+}]_i$ was calculated as 0.04, 6.0 and 0.02 nM for solutions containing 5 mM EGTA, 0.1 mM BAPTA and 30 mM BAPTA, respectively (WEBMAXC v2.22; http://stanford.edu/~cpatton/maxc.html). To block all K^+ currents for measurement of Ca^{2+} or Sr^{2+} currents, KCl was replaced by CsCl.

For outside-out patch recordings, the standard pipette solution was used for Ca_i^{2+}-free conditions. For increased $[Ca^{2+}]_i$, EGTA was replaced by 2 mM lower-affinity buffer di-bromo-BAPTA (K_D for Ca^{2+}, 1.8 μM at 23°C and pH 7.3; Fluka). Appropriate amounts of Ca^{2+} (0.706, 1.232 and 1.700 mM $CaCl_2$) were added to yield free $[Ca^{2+}]_i$ of 1, 3 or 10 μM $[Ca^{2+}]_i$, respectively; this was checked with Ca^{2+}-sensitive electrodes and adjusted if necessary. For outside-out recordings with 1 or 10 μM intracellular Sr^{2+}, 5 mM EDTA was used as the buffer (K_D for Sr^{2+}, 2.6 μM) and 1.355 or 3.949 mM $SrCl_2$ was added, respectively. As K_D values for Mg^{2+} and Sr^{2+} are approximately the same, Mg^{2+} and ATP were omitted from these pipette solutions and replaced by equal amounts of KCl. To obtain 100 μM Sr^{2+}, $SrCl_2$ was added without buffering.

For inside-out patches, pipettes were filled with standard extracellular solution. After excision, patches were placed in front of an array of capillaries that allowed exchange between solutions with different free $[Ca^{2+}]_i$. Composition of these solutions was as follows (mM): KCl 135, $MgCl_2$ 1, Hepes 5 and 4-AP 10; pH adjusted to 7.3 with HCl. Free $[Ca^{2+}]$ was buffered with 2 mM di-bromo-BAPTA to 1, 3 and 10 μM by adding 0.706, 1.232 and 1.700 mM $CaCl_2$, respectively. For 0 $[Ca^{2+}]$, the solution contained 5 mM EGTA instead of di-bromo-BAPTA. Free $[Ca^{2+}]$ was verified with Ca^{2+}-sensitive electrodes.

XE991 (DuPont, Wilmington, DE, USA), isradipine (kindly provided by T. Moser, Göttingen), ryanodine (Calbiochem, Bad Soden, Germany, or Tocris, Ellisville, MO, USA), cyclopiazonic acid (CPA; Calbiochem), 2,5-di-(t-butyl)-1,4-hydroquinone (BHQ; Calbiochem) and carboxy-eosine (Molecular Probes) were prepared as stock solutions in DMSO. XE991, isradipine, ryanodine, CPA and BHQ were added to the extracellular solution and carboxy-eosine to the pipette solution yielding final DMSO concentrations of 0.1%.

Giant patch recordings from *Xenopus* oocytes

Harvesting of *Xenopus* oocytes, mRNA injection and giant patch-clamp recordings were done as previously described (Oliver *et al.* 2000). Briefly, mRNA coding for mouse BKα (Accession No. A48206) was injected into isolated oocytes. Giant inside-out patches were excised using patch pipettes of ~0.3 MΩ filled with (mM): NaCl 115, KCl 5, $CaCl_2$ 1 and Hepes 10 (pH 7.2). For activation curves shown in Fig. 1*E*, patches were perfused with intracellular solution containing 100 mM KCl, 10 mM K_2-EGTA and 10 mM Hepes (pH 7.2). For experiments with varying Ca^{2+} buffer (0.1 *versus* 30 mM BAPTA), solutions applied to the patches were identical to the respective intracellular solutions used for IHCs.

Data analysis

Data analysis and fitting was performed with IgorPro (WaveMetrics, Lake Oswego, OR, USA) on a Macintosh PowerPC. All reported voltages (i.e. at steady-state current) were corrected off-line for measured liquid junction potentials and for voltage errors arising from voltage drop across the residual series resistance.

Activation curves of BK_{Ca} were determined using tail-current voltage protocols composed of brief prepulses (usually 5 ms) to minimize activation of residual slow outward currents, followed by a fixed tail potential (see Results). Tail-current amplitudes were plotted *versus* the corrected prepulse potential for each cell or patch; activation curves were fitted with a first-order Boltzmann function:

$$I = I_{leak} + I_{max}/(1 + \exp((V - V_h)/\alpha)),$$

where I_{leak} is voltage-independent leak current, I_{max} is the amplitude of the fully activated current at the tail-current potential, V is the prepulse voltage, V_h is the voltage at half-maximal activation and α is the slope factor. I_{leak} was subtracted, and currents were normalized to I_{max} for each experiment. All data are presented as means ± S.E.M. Activation curves displayed in the figures are averaged from normalized data of n experiments and the presented fitted curves show the fits to the averaged data. Values given in the figure legends refer to fits to the averaged data whereas data given in the text represent means ± S.E.M. of the values from individual cells or patches. Horizontal error bars for voltages are smaller than the symbol size in the activation curves. Statistical significance of differences between two sets of individual measurements was assessed with the Kolmogorov-Smirnov test that does not presuppose normal distribution of the data.

Results

Hair cell $I_{K,f}$ is mediated by BK_{Ca} channels

Mature mammalian IHCs display two major outwardly rectifying K^+ conductances that differ in their activation kinetics. A fast component, $I_{K,f}$, activates with submillisecond kinetics and a slower component,

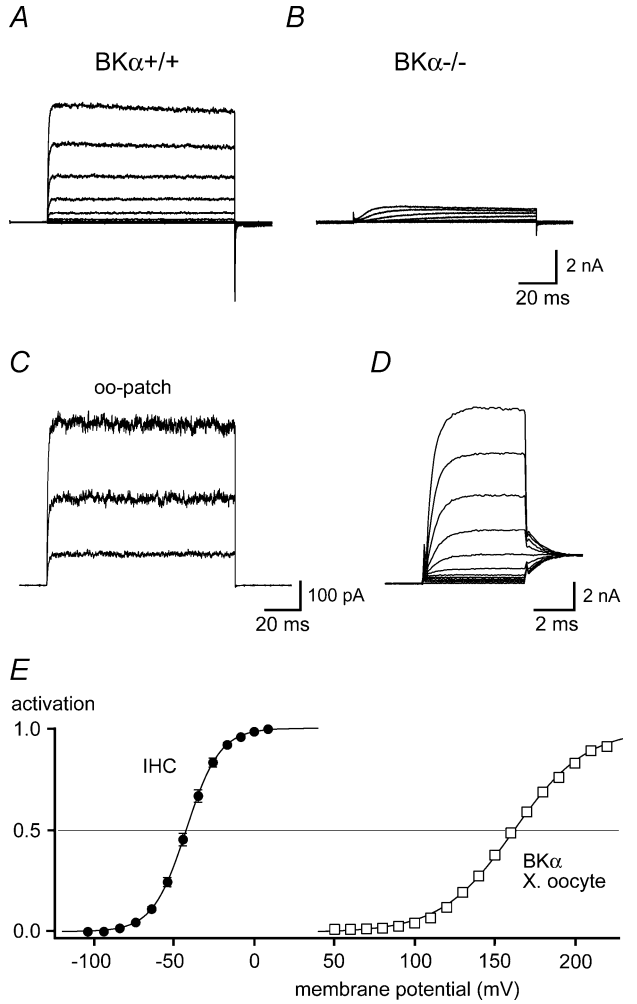

Figure 1. $I_{K,f}$ is mediated by BK_{Ca} channels
A and *B*, outwardly rectifying K^+ currents recorded in IHCs from a BKα knock-out mouse (BK$\alpha-/-$; *B*) and a littermate control (BK$\alpha+/+$; *A*). Currents were recorded in whole-cell mode in response to voltage steps to potentials between −104 and +6 mV (10 mV nominal increments) from a holding potential of −84 mV. Intracellular and extracellular solution contained 10 mM 4-AP and 1 μM XE991, respectively (see Methods). Note that the fast activating $I_{K,f}$ was absent in the BK$\alpha-/-$ IHC, where only a minor residual, slowly activating K^+ current component was observed. *C*, BK currents recorded in an outside-out patch excised from a rat IHC. Current traces were evoked by voltage steps to +16, +56 and +96 mV, from a holding potential of −64 mV. Solutions were as in (*A* and *B*). Each trace is averaged from 10 individual presentations of the voltage step. *D*, fast activation of $I_{K,f}$ in a rat IHC, recorded as in *A* in response to 5-ms steps incremented by nominally 10 mV. Tail-current potential was −34 mV. Monoexponential fits to the current activation (not shown) yielded a time constant ($\tau_{activation}$) between 0.67 ms (at −44 mV) and 0.37 ms (at +6 mV). *E*, steady-state activation curve determined from tail currents measured in 16 rat IHCs as in *C*. Currents were normalized to the saturating tail-current amplitude and plotted *versus* the prepulse potential corrected for errors resulting from residual series resistance (see Methods); standard error of the voltage was smaller than the symbol size. The continuous line is a fit of a first-order Boltzmann function to the averaged data, yielding values for V_h and α of −42.4 mV and 10.4 mV, respectively. For comparison of the activation voltage ranges, activation curves obtained in excised patches from BK_{Ca}-expressing *Xenopus* oocytes at 0 $[Ca^{2+}]_i$ are shown (□; mean data from seven patches; error bars are smaller than symbol size). The continuous line through the recombinant data (*Xenopus* oocyte) is a Boltzmann fit to the averaged data, yielding values for V_h and α of 161.9 mV and 22.6 mV, respectively.

$I_{K,s}$, shows strongly voltage-dependent activation kinetics with time constants of several milliseconds (Kros & Crawford, 1990). A third K^+ current is activated at hyperpolarized potentials and carried by KCNQ channels (Oliver *et al.* 2003). The currents can be separated pharmacologically and the sensitivity of the fast component to TEA, charybdotoxin and iberiotoxin strongly suggests that it is carried by BK_{Ca} channels (Kros *et al.* 1998; Raybould *et al.* 2001; Skinner *et al.* 2003; Marcotti *et al.* 2004). However, some ambiguity about the identity of $I_{K,f}$ remained given its apparent independence of calcium influx (Kros & Crawford, 1990; Marcotti *et al.* 2004).

Figure 1*A* and *B* shows whole-cell recordings obtained in IHCs from either a BKα knock-out (BK$\alpha-/-$; Sausbier *et al.* 2004) or a littermate wild-type mouse (BK$\alpha+/+$). In both experiments, slow potassium currents were blocked with 10 mM 4-AP and 1 μM XE991 (Kros & Crawford, 1990; Oliver *et al.* 2003; Marcotti *et al.* 2004). In wild-type IHCs, depolarization elicited the fast-activating, non-inactivating outward current $I_{K,f}$ that was absent in cells from BK$\alpha-/-$ mice ($n = 12$). This result unequivocally identified $I_{K,f}$ as a BK_{Ca}-mediated current. Moreover, only a small residual outward current with slow activation kinetics remained in the BK$\alpha-/-$ cells in the presence of 4-AP and XE991; these recordings thus confirmed that BK_{Ca} currents can be adequately isolated with these channel blockers and short depolarizing pulses.

BK_{Ca} currents displayed rapid onset at voltages positive to −60 mV with time constants between 0.7 and 0.4 ms (Fig. 1*D*). Inactivation of BK_{Ca} currents was not observed (Fig. 1*A*). However, as IHC currents are very large, especially when not separated pharmacologically, recordings are prone to series resistance-dependent voltage errors that vary with time as the currents activate (Marcotti *et al.* 2004). Such voltage errors may distort the apparent current kinetics. BK currents recorded in excised patches are much smaller and do not suffer from this problem. Patch recordings (Fig. 1*C*) showed the same kinetic properties of BK, confirming the proper isolation of BK in the whole-cell recordings, and in particular the absence of inactivation. Whole-cell steady-state activation was determined from tail currents following 5-ms steps to potentials between −104 mV and 6 mV. Fitting these activation curves with a Boltzmann function (see Methods) yielded a mean V_h value of -41.8 ± 0.3 mV ($n = 16$) and a slope factor of 10.3 ± 0.3 mV (Fig. 1*E*),

similar to the values previously published for $I_{K,f}$ in guinea pig (Kros & Crawford, 1990) and mouse (Oliver *et al.* 2003; Marcotti *et al.* 2004). This very negative steady-state activation obtained in whole IHCs under physiological conditions was strikingly different from channel activation determined under Ca^{2+}-free conditions in patches excised from *Xenopus* oocytes that expressed the α-subunit of the IHC BK_{Ca} channels (Langer *et al.* 2003). These recombinant BK_{Ca} channels activated with a V_h of 162.1 ± 2.4 mV and a slope factor of 21.9 ± 3.2 mV at 0 $[Ca^{2+}]_i$ (estimated free $[Ca^{2+}]_i$, 0.04 nM, see Methods; $n = 7$). The difference in activation of about 200 mV would be consistent with the IHC BK_{Ca} being gated by both transmembrane voltage and increased $[Ca^{2+}]_i$ (Oliver *et al.* 2003; Marcotti *et al.* 2004).

Ca^{2+}- and voltage-dependence of BK_{Ca} channels in excised IHC patches

The contribution of both factors was investigated by probing Ca^{2+}- and voltage-dependence of BK_{Ca} gating in excised patches from IHCs, allowing for a precise control of $[Ca^{2+}]_i$. Patches from rat IHCs typically harboured many BK_{Ca} channels yielding large ensemble K^+ currents (Fig. 2*A*). In both outside-out (Fig. 2*B*) and inside-out configurations (Fig. 2*C*), voltage-driven activation of currents was dependent on $[Ca^{2+}]_i$ with increasing $[Ca^{2+}]_i$ leading to a leftward shift of the activation curve. At 0 $[Ca^{2+}]_i$, V_h was 10.8 ± 5.9 mV and -15.2 ± 3.0 mV for inside-out ($n = 11$) and outside-out ($n = 5$) patches, respectively (Fig. 2*D*). Notably, these values for V_h at 0 $[Ca^{2+}]_i$ were much more negative than those reported for both native and recombinant BK_{Ca} channels (e.g. Tseng-Crank *et al.* 1994; Xie & McCobb, 1998; Jones *et al.* 1999), but were still more positive than V_h values determined in whole IHCs (−41.8 mV; Fig. 1*D*). Thus, channel activation approached the whole-cell V_h value at micromolar levels of $[Ca^{2+}]_i$ (~3 μM) at the cytoplasmic face of the excised patches. The slope of voltage dependence (α) was essentially constant throughout all Ca^{2+} concentrations tested.

Next we examined the activation kinetics and their dependence on $[Ca^{2+}]_i$ in excised patches (Fig. 2*F*). Activation time constants ($\tau_{activation}$) in inside-out patches were close to 1 ms at 0 $[Ca^{2+}]_i$, slightly slower at 1 μM, and faster at higher $[Ca^{2+}]_i$. Similar results were obtained in outside-out patches (Fig. 2*E*), but with a smaller effect of the lower Ca^{2+} concentrations on time constants, especially at positive potentials. Note that fast activation time constants equivalent to the rapid kinetics obtained in the whole-cell configuration (< 1 ms) required $[Ca^{2+}]_i$ of between 3 and 10 μM.

In conclusion, both the V_h and kinetics of BK_{Ca} activation in excised IHC patches in the presence of micromolar $[Ca^{2+}]_i$ are similar to the whole cell BK_{Ca} currents. However, the voltage dependence of the whole-cell currents is significantly steeper (~10 mV per e-fold change in voltage) than that determined for currents in isolated patches (~20 mV). As suggested previously, such voltage dependence may be due to a steeply voltage-dependent elevation of $[Ca^{2+}]_i$ in the intact IHC (Oliver *et al.* 2003).

Gating of BK_{Ca} channels in whole IHCs is independent of local increase in $[Ca^{2+}]_i$

To test this interpretation, we next performed experiments that manipulated the intracellular and extracellular Ca^{2+} concentration ($[Ca^{2+}]_{ex}$) while measuring BK_{Ca} currents in the whole-cell configuration.

Removal of extracellular Ca^{2+} (buffered with 5 mM BAPTA) abolished the Ca^{2+} current of IHCs (Fig. 3*A*, inset) and thus voltage-dependent influx via Cav. However, neither voltage-dependent activation of BK_{Ca} nor the maximal BK_{Ca} current recorded at −4 mV were significantly altered (Fig. 3*A*). This is in agreement with previous reports (Kros & Crawford, 1990; Marcotti *et al.* 2004). Also, blocking the IHC Cav channels with isradipine (10 μM; Platzer *et al.* 2000; Koschak *et al.* 2001) had no effect on the activation curve and the amplitude of the BK_{Ca} currents (Fig. 3*B*). These results suggested, that voltage-dependent Ca^{2+} influx is not involved in BK_{Ca} gating in IHCs.

This conclusion was further supported by experiments that replaced Ca^{2+} by the divalent Sr^{2+} which is able to substitute for Ca^{2+} in activating BK_{Ca} channels (Fig. 3*C*) and readily permeates the IHC Cav channels (Fig. 3*D*). Increasing intracellular Sr^{2+} concentration ($[Sr^{2+}]_i$) caused a leftward shift of the BK_{Ca} activation curve in excised outside-out patches (Fig. 3*C*), similar to the action of Ca^{2+}. However, Sr^{2+} was about 10-times less effective than Ca^{2+}, as 100 μM $[Sr^{2+}]_i$ shifted the V_h to −95 mV, while a V_h of −109 mV was obtained with 10 μM $[Ca^{2+}]_i$ (Fig. 3*C*). Equivalent results were obtained with recombinant BK_{Ca} channels expressed in *Xenopus* oocytes and investigated in giant inside-out patches (data not shown). In contrast to the large difference in activation potency, both divalent cations permeated equally well through the Cav channels of IHCs. Thus voltage-dependent inward currents recorded after blockade of all K^+ currents were similar in amplitude in the presence of 1.3 mM extracellular Ca^{2+} or Sr^{2+} (Fig. 3*D*). These findings predicted that if BK_{Ca} gating in whole IHCs required the influx of a divalent cation, replacement of extracellular Ca^{2+} by Sr^{2+} should lead to a shift of the activation curve to more positive values due to the lower efficiency of the inflowing Sr^{2+}; however, this was not observed. Instead, with Sr^{2+} as the permeating divalent cation, the BK_{Ca} activation curve appeared slightly shifted

to the left (Fig. 3*E* and *F*). This shift may be explained by a surface charge effect, as a similar shift in peak current is apparent in the current–voltage relation of the Ca^{2+} current (Fig. 3*D*).

Together, these results indicate that voltage-dependent Ca^{2+}influx is not involved in the gating of BK_{Ca} in IHCs and question whether BK_{Ca} channels in whole IHCs are sensitive to a rise in $[Ca^{2+}]_i$ at all. As IHCs are equipped with efficient Ca^{2+} clearing mechanisms (Kennedy, 2002), it appeared difficult to achieve a well-defined Ca^{2+} elevation via the whole-cell pipette without an exceedingly high free $[Ca^{2+}]$ in the pipette. We therefore used carboxy-eosin (50 μM; Gatto & Milanick, 1993), a blocker of plasma membrane Ca^{2+} ATPases,

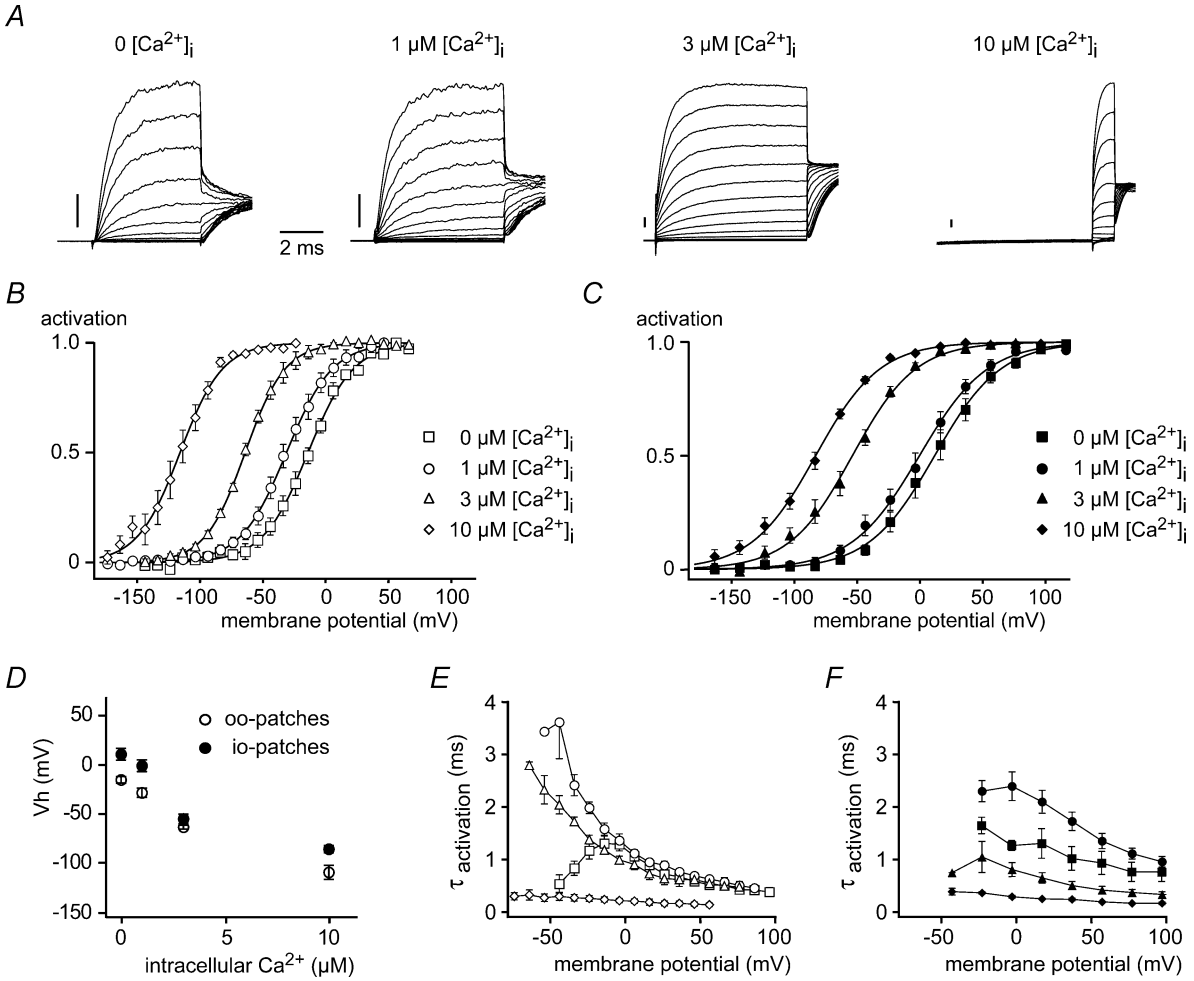

Figure 2. Ca^{2+}- and voltage-dependence of BK_{Ca} channels in patches excised from rat IHCs
A, BK_{Ca} currents recorded in outside-out patches from IHCs at the free $[Ca^{2+}]_i$ indicated. Holding potential was −83 mV, currents were elicited by step depolarizations to potentials between −143 and +37 mV (10-mV increments). Tail potential was −3 mV for 0, 1 and 3 μM and −37 mV for 10 μM $[Ca^{2+}]_i$. Each trace is averaged from 20 repetitions. Current scale bar, 0.2 nA. *B*, steady-state activation curves determined by tail-current analysis from outside-out patch recordings as in *A*. Free $[Ca^{2+}]_i$ in the pipette was as indicated, and data points show mean values of 5, 6, 4 and 11 patches for 0, 1, 3 and 10 μM $[Ca^{2+}]_i$, respectively. Continuous lines show Boltzmann fits to the averaged data. V_h and α were −14.1 mV and 18.1 mV (0 μM), −31.2 mV and 18.3 mV (1 μM), −64.1 mV and 15.9 mV (3 μM), −115.9 mV and 16.9 mV (10 μM $[Ca^{2+}]_i$), respectively. *C*, steady-state activation curves obtained from inside-out patches as in *B*. The indicated $[Ca^{2+}]_i$ was applied to the cytoplasmic face of the patches via a multibarrel pipette, data points are mean values of 9, 9, 9 and 11 patches for 0, 1, 3 and 10 μM $[Ca^{2+}]_i$, respectively. Continuous lines are Boltzmann fits to the averaged data. V_h and α were −11.6 and 26.3 mV (0 μM), −0.5 mV and 27.0 mV (1 μM), −53.9 mV and 25.2 mV (3 μM) and −83.2 mV and 25.5 mV (10 μM $[Ca^{2+}]_i$), respectively. *D*, summary of the V_h as a function of $[Ca^{2+}]_i$ for outside-out (○) and inside-out patches (●). *E*, activation time constants obtained from monoexponential fits to the rising phase of BK_{Ca} currents plotted against the membrane potential. Data are from the same outside-out patches analysed in *B*, symbols indicate values obtained with 0, 1, 3 and 10 μM $[Ca^{2+}]_i$ as in *B*. *F*, $\tau_{activation}$ of inside-out patches from *C* at the various $[Ca^{2+}]_i$ indicated by the symbols used in *C*.

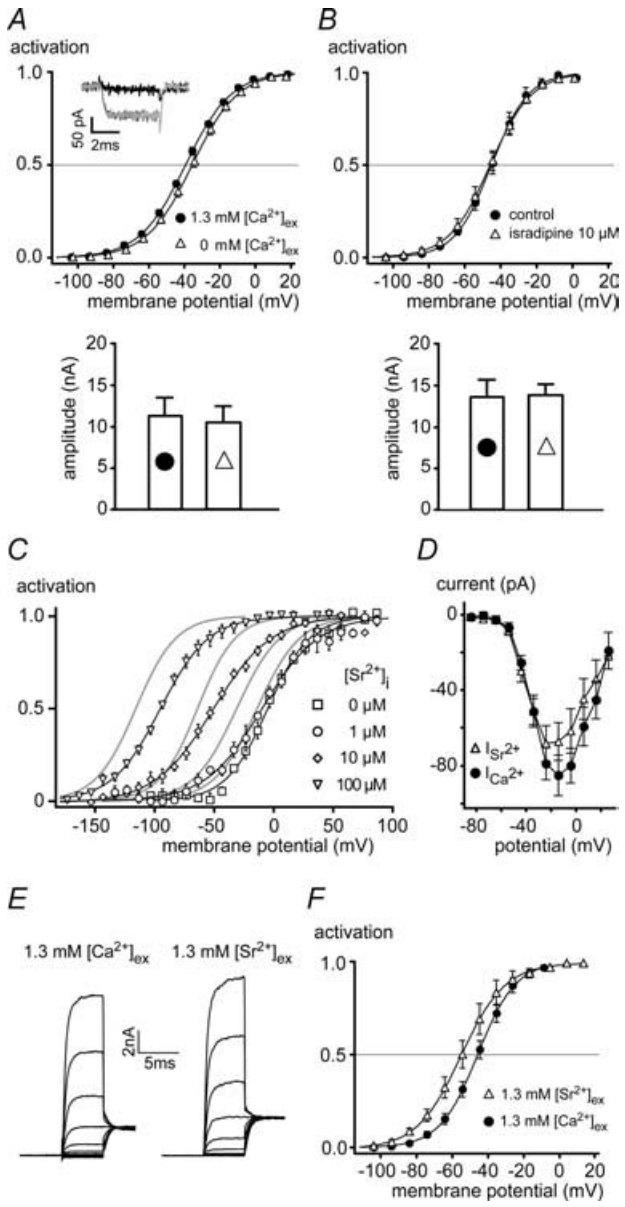

Figure 3. Ca^{2+} influx through Cav channels is not required for BK_{Ca} gating in IHCs

A, upper panel shows steady-state activation curves of BK_{Ca} channels measured in whole-cell mode in rat IHCs before and after withdrawal of extracellular Ca^{2+} (5 mM extracellular BAPTA). Continuous lines show Boltzmann fits to the averaged data yielding V_h and α of −39.3 mV and 12.9 mV with 1.3 mM Ca^{2+}, and −35.6 mV and 12.9 mV after withdrawal of extracellular Ca^{2+}, respectively. V_h values were not significantly different ($P = 0.45$; V_h values of individual experiments were −39.0 ± 1.0 mV (1.3 mM Ca^{2+}, $n = 6$) and −35.0 ± 2.0 mV (Ca^{2+}-free, $n = 6$). Inset, the Ca^{2+}-current in response to a step to −24 mV measured with a CsCl-based pipette solution was abolished by application of the Ca^{2+}-free extracellular solution (dark grey, control; black, 0 $[Ca^{2+}]_{ex}$; light grey, wash). Lower panel shows that the absolute BK_{Ca} current amplitude was not changed by removal of extracellular Ca^{2+}. Bars represent mean currents at −4 mV, where whole-cell activation was complete. *B*, upper panel show steady-state activation curves of BK_{Ca} channels measured in whole-cell mode in IHCs before and after block of Cav channels with isradipine (10 μM). Continuous lines show Boltzmann fits to the averaged data yielding V_h of −45.8 mV in the presence of isradipine ($n = 7$) and V_h of −45.1 mV in control conditions ($n = 7$). Slope factor α was 11.6 and 10.2 mV with and without isradipine, respectively. V_h values obtained from fits to individual experiments were not significantly different between both conditions ($P = 0.20$). Lower panel shows that current amplitude at −4 mV was not changed by application of isradipine. Currents in *A* and *B* (lower panels) were corrected for errors resulting from voltage drop across the residual series resistance (see Marcotti *et al.* 2004). *C*, BK_{Ca} currents measured in outside-out patches excised from IHCs were sensitive to $[Sr^{2+}]_i$. Steady-state activation curves at the $[Sr^{2+}]_i$ indicated were obtained as in Fig. 2*B* and fitted with a Boltzmann function (continuous lines). At 0, 1, 10 and 100 μM $[Sr^{2+}]_i$, values for V_h and α of BK_{Ca} activation were −5.5 mV and 17.6 mV ($n = 4$), −10.2 mV and 23.6 mV ($n = 3$), −51.4 mV and 24.6 mV ($n = 4$) and −95.6 mV and 20.3 mV ($n = 3$), respectively. Activation curves obtained with 0, 1, 3 and 10 μM $[Ca^{2+}]_i$ are shown for comparison (grey lines). Note that Sr^{2+} was about 10-fold less effective than Ca^{2+}. *D*, inward currents through Cav channels measured in whole-cell mode with extracellular solutions containing either 1.3 mM Ca^{2+} ($n = 5$ IHCs) or 1.3 mM Sr^{2+} ($n = 4$). Currents were recorded upon depolarizing voltage steps from a holding potential of −84 mV. CsCl-based pipette solution was used and extracellular solution contained 35 mM TEA to block all K^+ currents. *E*, whole-cell BK_{Ca} currents measured from the same IHC either at 1.3 mM $[Ca^{2+}]_{ex}$ (left-hand panel) or 1.3 mM $[Sr^{2+}]_{ex}$ (right-hand panel). Voltage protocol as in Fig. 1*C*. *F*, steady-state activation of BK_{Ca} channels determined from six experiments as in *E*. Lines are results of Boltzmann fits yielding values for V_h and α of −55.1 mV and 12.4 mV for 1.3 mM $[Sr^{2+}]_{ex}$, and −45.8 mV and 10.6 mV for 1.3 mM $[Ca^{2+}]_{ex}$, respectively.

to induce a global rise in $[Ca^{2+}]_i$. In the presence of carboxy-eosin and 5 mM EGTA in the patch pipette, the activation curve of BK_{Ca} currents steadily shifted to more negative potentials (average slope, 2.1 mV min^{-1}), reaching a V_h of about −100 mV after 25 min (Fig. 4*A*). In contrast, V_h remained constant over 30 min in the absence of carboxy-eosin (Fig. 4*A*). When Ca^{2+} clearance via the patch pipette was lowered by a 10-fold reduction in the buffer concentration (to 0.5 mM EGTA), the shift of V_h was considerably accelerated to 4.6 mV min^{-1}. Removal of extracellular Na^+ further accelerated the shift to 9.2 mV min^{-1}, most probably by inhibiting Na^+–Ca^{2+} exchange activity (Fig. 4*A*).

Ca^{2+} pumps are selective for Ca^{2+} over other divalent cations (Graf *et al.* 1982). We therefore investigated the behaviour of BK_{Ca} channels in response to prolonged influx of Sr^{2+} through the Cav channels activated repetitively by 500-ms depolarizations to −44 mV (Fig. 4*B*). Under these conditions, BK_{Ca} currents increased over time even at −44 mV and were fully activated at this voltage after several subsequent depolarizations (Fig. 4*D*). In contrast, such activation was not observed with extracellular Ca^{2+} (Fig. 4*C*) or after removal of extracellular Sr^{2+} (Fig. 4*E*) indicating that a global increase in $[Sr^{2+}]_i$ was able to activate BK_{Ca} channels in the whole-cell configuration.

These findings show that Ca^{2+} influx through Cav channels does not activate BK_{Ca} channels in the intact

IHC, although BK_{Ca} channels are perfectly sensitive to a global increase in cytoplasmic concentration of Ca^{2+} (and Sr^{2+}). It appeared therefore most likely that Cav channels are not tightly enough colocalized with BK_{Ca} to provide a sufficiently high increase in local $[Ca^{2+}]_i$.

Such a local increase in $[Ca^{2+}]_i$ may, however, be provided by Ca^{2+} released from internal stores and thus explain the difference in activation range observed between BK_{Ca} channels in whole-cell and excised patch recordings at 0 $[Ca^{2+}]_i$ (Marcotti *et al.* 2004). To test this possibility, the endoplasmic reticulum Ca^{2+} pump (SERCA) was blocked with a saturating concentration of the inhibitor cyclopiazonic acid (CPA; 50 μM). Inhibition of SERCA will deplete intracellular Ca^{2+} stores (Mason *et al.* 1991) and inhibit processes that depend on Ca^{2+} release. In the presence of CPA the IHCs were repetitively depolarized to accelerate any putative Ca^{2+} efflux from stores and induce their depletion. However as shown in Fig. 5*A* and *B* neither the V_h and slope of the BK_{Ca} activation curve, nor the current amplitude were altered significantly even after prolonged application of CPA. The values for V_h before and during application of CPA (10 min) were -38.6 ± 1.6 mV ($n = 3$) and -41.7 ± 1.1 mV ($n = 7$), respectively ($P = 0.31$). In addition, BHQ (100 μM; Mason *et al.* 1991), a chemically unrelated SERCA inhibitor, also failed to change the BK_{Ca} activation properties. After BHQ application (3–10 min) V_h was -41.1 ± 1.7 mV in five IHCs, which had a V_h of -37.7 ± 2.8 mV prior to BHQ application. Furthermore, the involvement of Ca^{2+} release was probed by blocking putative release channels.

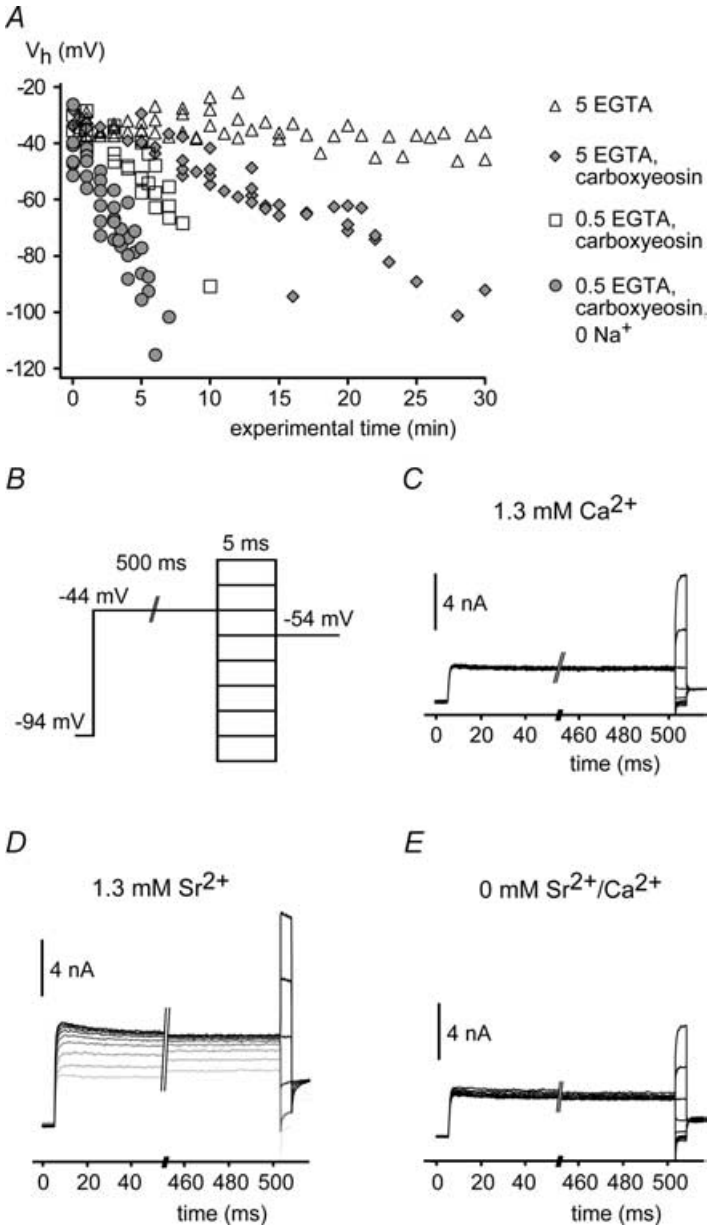

Figure 4. BK_{Ca} channels in intact IHCs are sensitive to a global increase in $[Ca^{2+}]_i$
A, activation of BK_{Ca} currents measured in whole-cell mode in IHCs under various conditions interfering with Ca^{2+} extrusion. V_h values were obtained from Boltzmann fits to the activation curves obtained as in Fig. 1*C* and plotted against the time after establishment of whole-cell access. V_h remained constant under control conditions (△; $n = 6$ IHCs) but shifted to more negative potentials when 50 μM carboxy-eosin was included in the pipette solution (◆; $n = 5$). Reduction of the intracellular Ca^{2+} buffer EGTA to 0.5 mM (□; $n = 5$) and replacement of external Na^+ by $NMDG^+$ (●; $n = 6$) further accelerated the leftward shift. Symbols show pooled data for each condition. Cells usually deteriorated when reaching a V_h of around −100 mV, precluding the observation of the BK_{Ca} activation curve beyond this value. *B*, voltage protocol for measuring BK_{Ca} currents with a depolarizing prepulse to −44 mV to allow for a prolonged inward current through Cav channels prior to each 5-ms test voltage step in nominal 10-mV increments. Intervals between successive sweeps were 55 ms. *C*, BK_{Ca} current response to the voltage protocol in *B* under control conditions with 1.3 mM $[Ca^{2+}]_{ex}$. *D*, BK_{Ca} current response from the same cell as in *C* after replacement of Ca^{2+} by Sr^{2+}. Note that the amplitude of the BK_{Ca} current increased during the prepulse with each voltage step. Consequently, currents during the short test voltage step were larger and were activated already at more negative potentials. The first sweep is shown in light grey; subsequent sweeps are shown in increasingly darker grey. *E*, BK_{Ca} current response as in *C* after removal of extracellular Sr^{2+}.

In immature IHCs, Ca^{2+} release via ryanodine receptors (RyRs) is involved in amplifying presynaptic Ca^{2+} signals (Kennedy & Meech, 2002). We therefore applied ryanodine (50 μM) which is known to block RyRs at micromolar concentrations (Meissner, 1986). Activation properties of BK_{Ca} were not changed significantly by ryanodine (5 min). Steady-state activation curves obtained with ryanodine and under control conditions yielded values for V_h and slope factor of -43.8 ± 2.8 mV and 10.3 ± 0.5 mV (ryanodine; $n = 5$) and -40.4 ± 1.4 mV and 10.0 ± 0.8 mV (control; $n = 5$), respectively. To ensure that intracellular concentrations were sufficiently high to block release channels we additionally applied ryanodine (30 μM; see Marcotti *et al.* 2004) through the patch pipette and measured BK activation curves 5–10 min after establishment of the whole-cell access. On average, V_h was slightly more positive in the presence of ryanodine (V_h, -33.3 ± 3.0 mV; α, 12.1 ± 0.6 mV; $n = 6$ IHCs) when compared to control cells from the same preparations without ryanodine (V_h, -38.9 ± 2.2 mV; α, 12.8 ± 0.5 mV; $n = 6$ IHCs); however, this difference was not statistically significant ($P = 0.45$). Current amplitudes with ryanodine (9.3 ± 1.8 nA at -14 mV) and in control IHCs (12.5 ± 1.2 nA) were also not significantly different ($P = 0.45$).

We next explored the involvement of local $[Ca^{2+}]_i$ in BK_{Ca} gating by using the fast Ca^{2+} buffer BAPTA at high (30 mM) and low concentrations (0.1 mM) in the

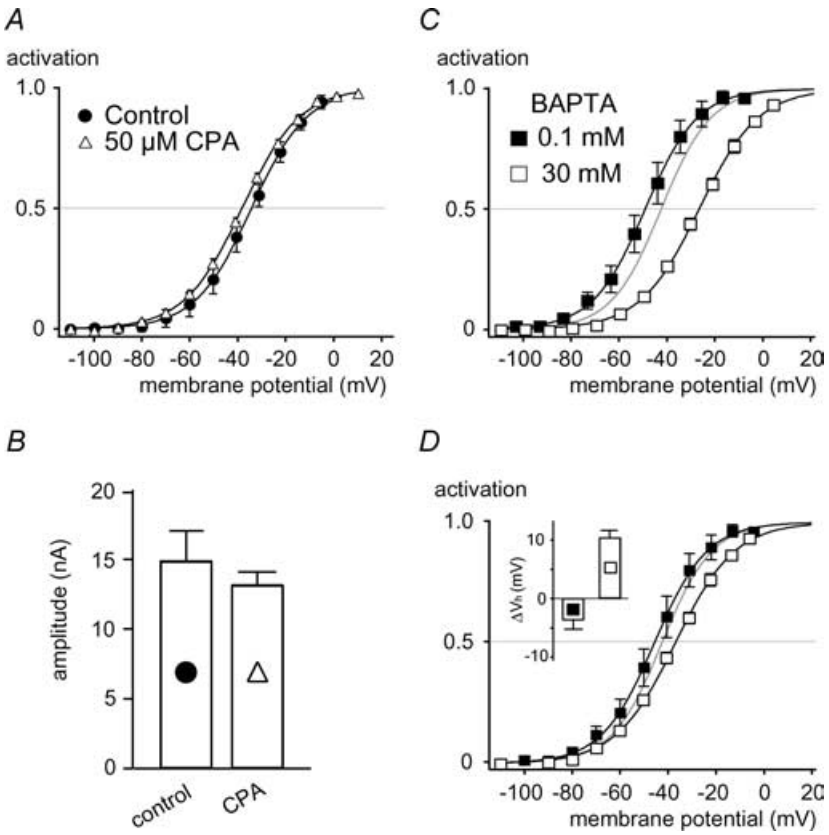

Figure 5. BK_{Ca} activation in IHCs does not require Ca^{2+} release from internal stores
A, activation curves measured before ($n = 3$) and after prolonged application (10 min) of the SERCA blocker CPA to IHCs (50 μM; $n = 7$). Boltzmann fits (continuous lines) to the averaged data (mean values of three experiments) yielded values for V_h and α of -34.4 mV and 11.7 mV for controls, and -38.2 mV and 12.1 mV with CPA, respectively. During application of CPA, the cell was depolarized repetitively to facilitate store depletion. *B*, absolute BK_{Ca} current amplitudes measured at +6 mV from the same cells shown in *A*. The difference between control and CPA was not significant ($P = 0.61$). Correction for series resistance error as in Fig. 3*A* and *B*. *C*, activation curves measured with pipette solutions containing either 0.1 ($n = 5$ IHCs) or 30 mM ($n = 6$) fast Ca^{2+} chelator BAPTA. Continuous lines indicate Boltzmann fits to the averaged data, yielding values for V_h and α of -49.1 and 11.0 mV for 0.1 mM BAPTA, and -26.5 mV and 12.3 mV for 30 mM BAPTA. Grey line represents the fit to control data (5 mM EGTA) from Fig. 1*D*. *D*, inset shows that intracellular BAPTA (0.1 and 30 mM) directly shifted BK_{Ca} activation curves measured in inside-out patches at 0 $[Ca^{2+}]_i$ to more negative or positive values, respectively, compared to 5 mM EGTA. Solutions applied to the cytoplasmic side of the patch were identical to the intracellular solutions used in *C*. Whole-cell activation curves for 0.1 (■) and 30 mM BAPTA (□) from *B* are shown with this direct effect of BAPTA subtracted. Boltzmann fits (continuous lines) to the corrected data yielded V_h and α values of -45.6 mV and 11.0 mV, and -36.8 mV and 12.3 mV for 0.1 and 30 mM BAPTA, respectively. Grey line represents activation curve at 5 mM EGTA as in *C*.

whole-cell pipette. Free $[Ca^{2+}]$ was subnanomolar in these pipette solutions, as no Ca^{2+} was added. BK_{Ca} activation curves were recorded only after complete equilibration of BAPTA with the cytoplasm; that is, more than 3 min after establishing whole-cell access. The effective buffer concentrations of the intracellular solutions were verified by titration using a Ca^{2+}-sensitive electrode and were found to match the respective BAPTA concentration within 10%. As shown in Fig. 5*C*, the V_h values obtained at 0.1 and 30 mM BAPTA were -47.5 ± 3.4 mV ($n = 5$) and -27.0 ± 1.4 mV ($n = 6$), respectively, which were significantly different from each other ($P = 0.009$), and V_h at 30 mM BAPTA significantly differed from measurements with 5 mM EGTA ($P = 0.0003$). In contrast to the V_h values, the slope factors of the activation curves recorded in 0.1 and 30 mM BAPTA were not significantly different from each other or from the measurement in the presence of EGTA (α, 10.7 ± 0.6 mV and 12.1 ± 0.5 mV for 0.1 and 30 mM BAPTA, respectively; $P = 0.52$).

As increasing BAPTA to 30 mM markedly changes the bulk ionic properties of the intracellular milieu (most monovalent anions are replaced by a much lower concentration of tetravalent ions), the BAPTA-containing solutions (without any added Ca^{2+}) were tested for direct effects on BK_{Ca} channels in inside-out patches excised either from IHCs or BK_{Ca}-expressing oocytes. These solutions contained less than 6 nM free $[Ca^{2+}]_i$ (see Methods), a concentration that does not activate BK channels even at very positive potentials (Cui *et al.* 1997). Thus, any change in BK activation observed with these solutions cannot be mediated by Ca^{2+}. As shown in Fig. 5*D* (inset), BK_{Ca} activation was shifted towards depolarized potentials by 10.3 ± 1.2 mV ($n = 7$ IHC patches) when the intracellular solution with 5 mM EGTA was changed to the solution containing 30 mM BAPTA. At 0.1 mM BAPTA, V_h was slightly shifted in the opposite, negative, direction by -3.6 ± 1.7 mV (Fig. 5*D*, inset). The slope factor was not affected. Similarly, a shift in V_h of 16.7 ± 4.0 mV ($n = 6$) was determined for heterologously expressed BK_{Ca} upon changing from 0.1 to 30 mM BAPTA. Thus, the concentration and species of the Ca^{2+} buffer influenced BK_{Ca} channel activation, but not by affecting the $[Ca^{2+}]_i$ sensed by the channels. Subtracting this 'non-specific' (not Ca^{2+}-mediated) effect of BAPTA from the V_h values determined in whole IHCs with 0.1 and 30 mM BAPTA, results in corrected V_h values of -44.0 and -37.3 mV, respectively. The corrected activation curves were close to the data obtained with the slow buffer EGTA in the pipette (Fig. 5*D*); the corrected V_h values for 0.1 and 30 mM BAPTA were not significantly different from the data obtained with EGTA ($P = 0.170$ and 0.167, respectively). Thus, the rightward shift observed upon application of BAPTA to IHCs was predominantly due to a direct effect of the buffer molecule on the BK_{Ca} properties rather than resulting from the buffering of local $[Ca^{2+}]_i$ in the vicinity of the channel.

Together, these experiments indicated that activation of IHC BK_{Ca} channels in the voltage range around -40 mV is not due to a local rise of $[Ca^{2+}]_i$ fuelled either by release of Ca^{2+} from internal stores or by Ca^{2+} influx through Cav channels. Instead, the negative activation range of $I_{K,f}$ appears to be an intrinsic property of the channel protein.

Gating of BK_{Ca} channels in IHCs of KCNMB1 knock-out mice

Voltage dependence of BK_{Ca} channels is modified by auxiliary β-subunits, the KCNMB1–4 proteins (McManus *et al.* 1995; Brenner *et al.* 2000*a*). BKβ1 (KCNMB1) is coexpressed with the pore-forming BKα subunit in mature IHCs (Langer *et al.* 2003). To assess the role of BKβ1, BK_{Ca} currents were measured in IHCs from mice with a targeted deletion of KCNMB1 (BKβ1−/−; Brenner *et al.* 2000*b*).

The voltage dependence of whole-cell BK_{Ca} currents recorded from BKβ1−/− IHCs (V_h, -45.0 ± 1.4 mV), was identical to currents from wild-type control mice (V_h, -45.7 ± 2.4 mV; Fig. 6*A*). Likewise, neither current amplitudes (Fig. 6*B*) nor activation time constants of BK_{Ca} (Fig. 6*C*) were changed substantially by ablation of BKβ1. In outside-out patches, BK_{Ca} currents from BKβ1−/− animals were indistinguishable from controls at 0 $[Ca^{2+}]_i$ (V_h, -0.7 ± 6.4 and 0.9 ± 10.4 mV, respectively; Fig. 6*D*). At 10 μM $[Ca^{2+}]_i$, BK_{Ca} channels from BKβ1−/− mice appeared to activate at potentials slightly more positive than those from control animals (Fig. 6*D*), although the difference was not statistically significant ($P = 0.24$). The activation kinetics of BK_{Ca} in patches were also not substantially different between wild-type and BKβ1−/− when measured at subnanomolar levels of $[Ca^{2+}]_i$ or with 10 μM $[Ca^{2+}]_i$ (Fig. 6*E*).

Unaltered properties of BK_{Ca} upon ablation of KCNMB1 obtained in excised patches and in the intact cell thus show that the negative activation range of BK_{Ca} currents in the IHCs is not due to association of BKα with the BKβ1 protein.

Discussion

Identity of $I_{K,f}$ and properties in excised patches

Several lines of evidence previously indicated that $I_{K,f}$, the fast activating K^+ conductance in IHCs, is carried by BK_{Ca} channels. This included sensitivity to the specific BK_{Ca} channel blockers iberiotoxin and charybdotoxin (Kros *et al.* 1998; Marcotti *et al.* 2004; Pyott *et al.* 2004; Hafidi *et al.* 2005), and the $[Ca^{2+}]_i$ dependence of its activation observed in excised inside-out patches (Oliver *et al.* 2003). Here we show that targeted deletion of the

pore-forming BK_{Ca} α-subunit abolished $I_{K,f}$ in IHCs, which unequivocally identifies $I_{K,f}$ as a BK_{Ca} current. The minor residual current component observed in IHCs from BKα−/− mice demonstrates that $I_{K,f}$ can be appropriately isolated with 4-AP in the patch pipette to block $I_{K,s}$ (Kros & Crawford, 1990) and XE991 to block the KCNQ-type $I_{K,n}$ (Oliver *et al.* 2003). Notably, this finding supports the non-inactivating nature of BK_{Ca} in IHCs as suggested previously (Oliver *et al.* 2003; Marcotti *et al.* 2004) but contrasts with a report showing inactivation of $I_{K,f}$ currents obtained by subtraction of pharmacologically isolated current components (Pyott *et al.* 2004). The absence of inactivation cannot be attributed to the 4-AP in our recording solution, because 4-AP does not affect the inactivation of BK channels (Armstrong & Roberts, 2001). Marcotti *et al.* (2004) argued that an apparent inactivation of $I_{K,f}$ may result from time-varying voltage errors that easily occur with the large IHC currents in the presence of even a moderate series resistance. The present recordings in isolated patches in the absence of series resistance problems and at very positive potentials (Fig. 1*C*; see Oliver *et al.* 2003) support this view.

Recordings in patches from rat (and mouse) IHCs revealed the signature behaviours of BK_{Ca} channels: (i) channel activation with a relatively shallow voltage dependence (α, ~20 mV); and (ii) the shift of the steady-state activation curve to hyperpolarized potentials with increasing $[Ca^{2+}]_i$. The most noteworthy observation obtained with patches is the very negative activation with V_h values of −15 mV and 11 mV even in the absence of free $[Ca^{2+}]_i$ (i.e. subnanomolar levels) in outside-out and inside-out patches, respectively. This negative activation

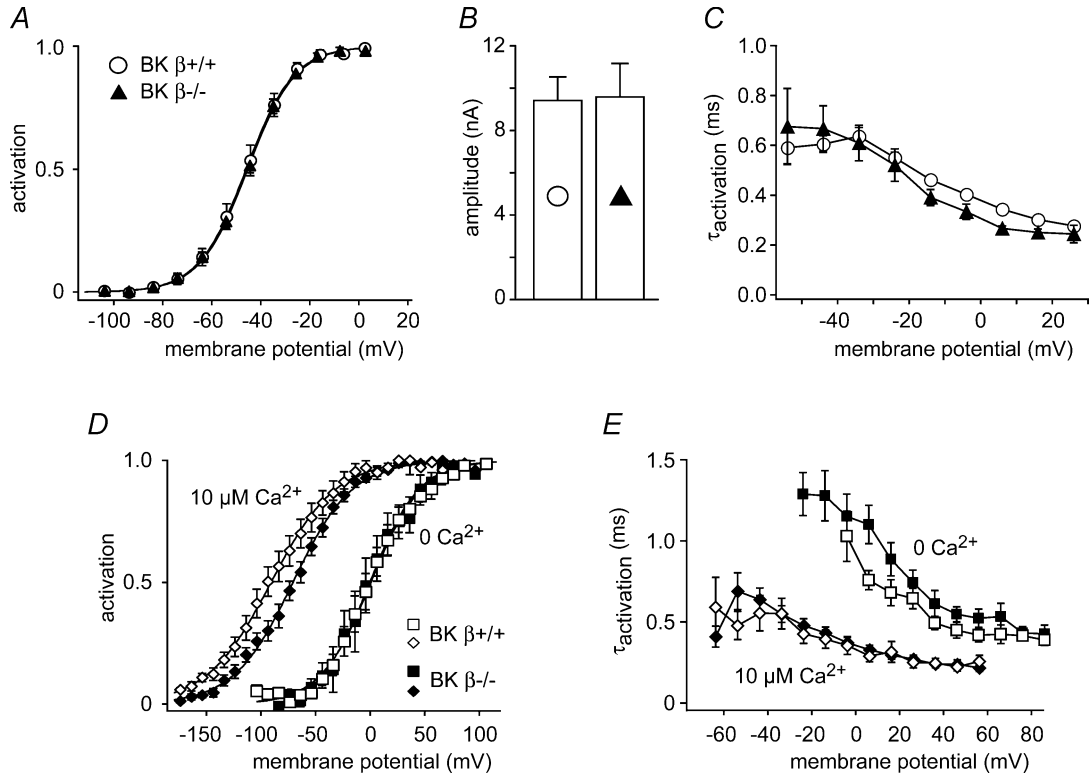

Figure 6. BK_{Ca} gating in IHCs is not affected by KCNMB1
A, steady-state BK_{Ca} activation curves determined from whole-cell recordings in IHCs of wild-type (○; $n = 7$) and BKβ1−/− mice (▲; $n = 9$). Lines represent results of Boltzmann fits to the averaged data yielding values for V_h and α of −45.5 mV and 9.7 mV for BKβ1−/− IHCs and −46.0 mV and 9.7 mV for wild-type IHCs, respectively. *B*, BK_{Ca} current amplitudes measured at −4 mV from the same IHCs as in *A* (symbols as in *A*). Currents were corrected for the voltage drop across the residual series resistance as in Fig. 3*A* and *B*. *C*, the time constants of activation, obtained from monoexponential fits to the rising phase of the same current data from *A* and *B* are very similar in BKβ1−/− and control IHCs (symbols as in *A*). *D*, BK_{Ca} activation measured in outside-out patches from wild-type and BKβ1−/− mice at 0 and 10 μM free $[Ca^{2+}]_i$ as in Fig. 2. Data are mean values of five and 14 patches for wild-type and eight and 16 patches for the BKβ1−/− IHCs. Lines represent results of a Boltzmann fit to the averaged data yielding values for V_h and α of −0.3 mV and 22.54 mV (wild-type at 0 Ca^{2+}), 0.6 mV and 23.0 mV (BKβ1−/− at 0 Ca^{2+}), −90.8 mV and 29.5 mV (wild-type at 10 μM 0 Ca^{2+}) and −70.7 mV and 27.2 mV (BKβ1−/− at 10 μM Ca^{2+}), respectively. *E*, activation time constants from the BK_{Ca} currents in *D* were essentially equal in BKβ1−/− and control patches, with only a slightly slower activation in BKβ1−/− at 0 Ca^{2+}. Time constants were obtained from monoexponential fits to the onset of the currents.

range was independent of Mg^{2+} which may also shift the voltage dependence of BK_{Ca} (Shi & Cui, 2001), as shown in Fig. 3*C* with EDTA-buffered intracellular solution. To our knowledge this is the most negative Ca^{2+}-independent activation voltage range described so far for BK_{Ca} currents from any type of cell (see Adelman *et al.* 1992; Tseng-Crank *et al.* 1994; McManus *et al.* 1995; Cui *et al.* 1997; Vergara *et al.* 1998; Jones *et al.* 1999; Brenner *et al.* 2000*a*).

A role for Ca^{2+} for activation of BK_{Ca} in the intact cell?

BK_{Ca} currents recorded from intact IHCs differ from patch currents at 0 $[Ca^{2+}]_i$ by their more negative range of activation (V_h, ∼−42 mV), faster kinetics ($\tau_{activation}$, 0.65 ms at room temperature; Fig. 1*C*; Marcotti *et al.* 2004), and steeper slope of the activation curve (α, ∼10 mV). These features would be most easily explained by an increase in $[Ca^{2+}]_i$. In particular, the steep slope factor suggested a voltage-dependent rise in $[Ca^{2+}]_i$ between −70 and −20 mV (Oliver *et al.* 2003) compatible with the Cav1.3 channels of IHCs (Platzer *et al.* 2000) that activate at exceptionally low voltages, similar to the activation range of $I_{K,f}$ (Xu & Lipscombe, 2001). In fact, this led us previously to suggest that Ca^{2+} influx via Cav1.3 may provide the increased $[Ca^{2+}]_i$ that could result in the particular activation properties of BK_{Ca} currents in IHCs (Oliver *et al.* 2003). The finding that targeted deletion of Cav1.3 abolished $I_{K,f}$ (Brandt *et al.* 2003), further supported this view.

However, the clear-cut finding that inhibition of Ca^{2+}-influx – either by removal/substitution of external Ca^{2+} or by blocking Cav channels – did not result in any alteration of the activation of BK_{Ca} channels, excludes this interpretation.

Our present data confirm previous reports that IHC BK_{Ca} channels are insensitive to changes in $[Ca^{2+}]_{ex}$ (Kros & Crawford, 1990; Marcotti *et al.* 2004). Moreover, we show that this does not indicate an intrinsic insensitivity for $[Ca^{2+}]_i$ in the intact IHC, as BK_{Ca} channels were effectively activated by an elevation of global $[Ca^{2+}]_i$ or $[Sr^{2+}]_i$ when extrusion of the divalent cation was blocked (Fig. 4). The lack of direct impact of Ca^{2+} influx strongly suggests that spatial separation of Cav and BK_{Ca} channels precludes functional coupling. This is consistent with the available data on localization of both channel types. Recent antibody staining showed that BK_{Ca} is predominantly located in large clusters along the apical segment of the lateral membrane of IHCs (Pyott *et al.* 2004; Ruttiger *et al.* 2004; Hafidi *et al.* 2005). Though clear immunohistochemical data on the subcellular distribution of Cav1.3 in mature IHCs are not yet available, these channels should be located at the basal presynaptic pole of the cells. Synaptic release at these sites depends on Ca^{2+} influx via Cav1.3 (Moser & Beutner, 2000; Brandt *et al.* 2003) and depolarization increases $[Ca^{2+}]_i$ close to the basal membrane in neonatal IHCs (Kennedy & Meech, 2002).

Alternatively, voltage dependence and onset kinetics of BK_{Ca} channels in IHCs may be set by Ca^{2+} released from internal stores (Marcotti *et al.* 2004). To address this issue we blocked Ca^{2+} release and Ca^{2+} reuptake to deplete stores and used high concentrations of the fast Ca^{2+} buffer BAPTA to diminish putative high local $[Ca^{2+}]_i$. All of these manipulations failed to significantly affect the amplitude or gating properties of BK_{Ca} currents (Fig. 5).

Some of these data stand in contrast to previous data (Marcotti *et al.* 2004) showing that manoeuvres thought to interfere with release of Ca^{2+} from internal stores shifted the activation curve to more positive potentials in mouse IHCs. A shift of the activation curve reported by Marcotti *et al.* (2004) for high concentrations of BAPTA was confirmed (Fig. 5), but demonstrated to result essentially from a Ca^{2+}-independent effect of the buffer molecule. Thus, application onto excised patches from either IHCs or *Xenopus* oocytes showed that increasing BAPTA concentration directly shifted BK_{Ca} activation by ∼10–15 mV in the absence of Ca^{2+}. Although a slight shift in V_h with intracellular ryanodine was in the same (depolarizing) direction as the shift reported by Marcotti *et al.* (2004), this effect was not significant. Extracellular application of ryanodine also did not produce a significant shift of the activation curves in our experiments. It is important to note that the shifts with store release blockers reported by Marcotti *et al.* (2004) were only moderate, yielding a V_h value not exceeding about −25 mV. Such an activation voltage is still more negative than observed in excised patches (Fig. 2) and is far more negative than the activation range of 'conventional' BK channels without elevated Ca^{2+} (e.g. Fig. 1*E*). Thus a contribution of Ca^{2+} released from internal stores can at most explain a minor part of the negative activation range, and a distinct mechanism must be present. This conclusion is fully consistent with the present data obtained from excised patches, a condition that excludes the contribution of store release and showed Ca^{2+}-independent activation well below 0 mV (Fig. 2).

Moreover, it appears unlikely that store-released Ca^{2+} can account for the fast and negative BK_{Ca} activation in IHCs for the following reasons. First, if $I_{K,f}$ properties depend on Ca^{2+} release, this release must be strongly voltage dependent to match the slope factor of ∼10 mV that exceeds the value in patches by about 2-fold. Accordingly, the stores would have to be operated by a voltage sensor in the plasma membrane, similar to the excitation–contraction coupling in skeletal muscle, where Cav1.1 channels physically interact with and gate sarcoplasmic reticulum ryanodine receptors (RyRs) (Lamb, 2000). However, all Cav channels in IHCs seem to be located distantly from BK_{Ca}. Second, manipulations that interfere with a Ca^{2+} store release should decrease

the voltage dependence of BK_{Ca}. Yet, the high slope factor is remarkably stable under all whole-cell conditions (Marcotti *et al.* 2004). Third, it is unlikely that the cascade of voltage sensor/RyR, release of Ca^{2+} and BK_{Ca} opening occurs in the submillisecond time range. Even in skeletal muscle, the delay between depolarization and Ca^{2+} release is reported to be of the order of a millisecond (Kim & Vergara, 1998), in contrast to the submillisecond kinetics of IHC BK_{Ca}.

Possible mechanisms that control BK_{Ca} gating phenotype

The apparent independence of BK_{Ca} channel activation on local $[Ca^{2+}]_i$ is consistent with a constitutive modification of the BK_{Ca} channel protein that endows the high voltage dependence, negative activation range and rapid kinetics of channel gating. This conclusion is supported by the finding of very negative activation of BK_{Ca} in patches excised from IHCs at precisely defined $[Ca^{2+}]_i$.

Such a modification may either occur pre/post-translationally or result from association with an auxiliary protein. Indeed, BK_{Ca} channel activation is reported to be modulated by a set of different mechanisms, including alternative splicing (Adelman *et al.* 1992; Tseng-Crank *et al.* 1994; Xie & McCobb, 1998), association with β-subunits (McManus *et al.* 1995; Brenner *et al.* 2000*a*) and protein phosphorylation (Reinhart *et al.* 1991; Schubert & Nelson, 2001). IHCs predominantly express minimal mRNA splice variants with conventional gating properties (Langer *et al.* 2003), and, to a lesser extent, a splice variant with a moderately increased Ca^{2+} sensitivity that, when expressed heterologously, still activates at markedly more positive potentials than IHC BK_{Ca} (Xie & McCobb, 1998; Ha *et al.* 2000). The known accessory β-subunits are unlikely to contribute to BK_{Ca} gating in IHCs. The BKβ1 knock-out failed to alter BK_{Ca} gating, a finding consistent with the lack of an obvious auditory phenotype in BKβ1−/− mice (Ruttiger *et al.* 2004). BKβ2 and β4, which may be expressed transiently in the immature organ of Corti (Langer *et al.* 2003), either endow channels with inactivation (β2; Wallner *et al.* 1999) or slow the kinetics (β1,2 and 4; Brenner *et al.* 2000*a*), properties that contrast with the observed characteristics of BK_{Ca} gating in IHCs. Expression of β3 in the cochlea has not been examined, but coexpression with β3 has little effect on kinetics and voltage dependence of BK_{Ca} gating (Brenner *et al.* 2000*a*), arguing against a role of β3 for the unusual behaviour of BK_{Ca} in IHCs. Activation of BK_{Ca} channels may be affected by the redox potential (DiChiara & Reinhart, 1997); however, our preliminary experiments with redox reagents (not shown) indicate that they have no effect on BK_{Ca} channels in excised patches from IHCs.

The different activation properties seen in whole-cell *versus* excised patch recordings suggest that the modulation of BK_{Ca} properties is at least partially reversible. Such dynamic behaviour may also underlie the difference between inside-out and outside-out patches and a substantially more negative V_h value in inside-out patches compared to similar data from mouse IHCs (Oliver *et al.* 2003). BK_{Ca} channel activation in outside-out patches more closely resembled the whole-cell situation, suggesting that a post-translational 'factor', perhaps a protein phosphorylation event that may confer rapid kinetics and hyperpolarized activation voltage onto the IHC BK_{Ca} channels, is lost in the inside-out configuration, but is better maintained in outside-out patches. In any case, the molecular nature of such modification, or the identity of a potentially BKα-associated auxiliary protein, remains to be elucidated.

In conclusion, we have shown that in IHCs BK_{Ca} channels are able to rapidly gate at negative membrane potentials without the requirement of an increase in $[Ca^{2+}]_i$, as necessary for BK_{Ca} function in other native cells. Instead, BK_{Ca} channels in IHCs effectively operate as purely voltage-gated outward rectifiers, essentially equivalent to Kv-type K^+ channels (e.g. Kv3.1, Kv1.1; Coetzee *et al.* 1999; Rudy *et al.* 1999), but with considerably faster activation and deactivation kinetics. Our conclusion challenges the concept that BK_{Ca} activation at physiological potentials generally requires micromolar $[Ca^{2+}]_i$. It will be interesting to see whether this mode of operation is also realized in other tissues, in particular neurones, where BK_{Ca} is involved in the regulation of firing patterns (e.g. Sausbier *et al.* 2004). It is important to note that in excised patches from IHCs the voltage dependence was shifted considerably to more depolarized potentials compared to the intact cell. Thus, recordings of BK_{Ca} currents in isolated patches do not necessarily faithfully report the voltage and Ca^{2+} dependence of the channels under physiological (whole-cell) conditions, and a Kv-like behaviour might easily be missed.

References

Adelman JP, Shen KZ, Kavanaugh MP, Warren RA, Wu YN, Lagrutta A, Bond CT & North RA (1992). Calcium-activated potassium channels expressed from cloned complementary DNAs. *Neuron* **9**, 209–216.

Armstrong CE & Roberts WM (2001). Rapidly inactivating and non-inactivating calcium-activated potassium currents in frog saccular hair cells. *J Physiol* **536**, 49–65.

Art JJ & Fettiplace R (1987). Variation of membrane properties in hair cells isolated from the turtle cochlea. *J Physiol* **385**, 207–242.

Art JJ, Fettiplace R & Wu YC (1993). The effects of low calcium on the voltage-dependent conductances involved in tuning of turtle hair cells. *J Physiol* **470**, 109–126.

Brandt A, Striessnig J & Moser T (2003). CaV1.3 channels are essential for development and presynaptic activity of cochlear inner hair cells. *J Neurosci* **23**, 10832–10840.

Brenner R, Jegla TJ, Wickenden A, Liu Y & Aldrich RW (2000*a*). Cloning and functional characterization of novel large conductance calcium-activated potassium channel beta subunits, hKCNMB3 and hKCNMB4. *J Biol Chem* **275**, 6453–6461.

Brenner R, Perez GJ, Bonev AD, Eckman DM, Kosek JC, Wiler SW, Patterson AJ, Nelson MT & Aldrich RW (2000*b*). Vasoregulation by the beta1 subunit of the calcium-activated potassium channel. *Nature* **407**, 870–876.

Coetzee WA, Amarillo Y, Chiu J, Chow A, Lau D, McCormack T *et al.* (1999). Molecular diversity of K^+ channels. *Ann N Y Acad Sci* **868**, 233–285.

Cui J, Cox DH & Aldrich RW (1997). Intrinsic voltage dependence and Ca^{2+} regulation of mslo large conductance Ca-activated K^+ channels. *J Gen Physiol* **109**, 647–673.

DiChiara TJ & Reinhart PH (1997). Redox modulation of hslo Ca^{2+}-activated K^+ channels. *J Neurosci* **17**, 4942–4955.

Fuchs PA, Nagai T & Evans MG (1988). Electrical tuning in hair cells isolated from the chick cochlea. *J Neurosci* **8**, 2460–2467.

Gatto C & Milanick MA (1993). Inhibition of the red blood cell calcium pump by eosin and other fluorescein analogues. *Am J Physiol* **264**, C1577–C1586.

Graf E, Verma AK, Gorski JP, Lopaschuk G, Niggli V, Zurini M, Carafoli E & Penniston JT (1982). Molecular properties of calcium-pumping ATPase from human erythrocytes. *Biochemistry* **21**, 4511–4516.

Ha TS, Jeong SY, Cho SW, Jeon H, Roh GS, Choi WS & Park CS (2000). Functional characteristics of two BKCa channel variants differentially expressed in rat brain tissues. *Eur J Biochem* **267**, 910–918.

Hafidi A, Beurg M & Dulon D (2005). Localization and developmental expression of BK channels in mammalian cochlear hair cells. *Neuroscience* **130**, 475–484.

Horrigan FT & Aldrich RW (2002). Coupling between voltage sensor activation, Ca^{2+} binding and channel opening in large conductance (BK) potassium channels. *J Gen Physiol* **120**, 267–305.

Hudspeth AJ & Lewis RS (1988*a*). Kinetic analysis of voltage- and ion-dependent conductances in saccular hair cells of the bull-frog, *Rana catesbeiana*. *J Physiol* **400**, 237–274.

Hudspeth AJ & Lewis RS (1988*b*). A model for electrical resonance and frequency tuning in saccular hair cells of the bull-frog, *Rana catesbeiana*. *J Physiol* **400**, 275–297.

Jones EM, Gray-Keller M & Fettiplace R (1999). The role of Ca^{2+}-activated K^+ channel spliced variants in the tonotopic organization of the turtle cochlea. *J Physiol* **518**, 653–665.

Kennedy HJ (2002). Intracellular calcium regulation in inner hair cells from neonatal mice. *Cell Calcium* **31**, 127–136.

Kennedy HJ & Meech RW (2002). Fast Ca^{2+} signals at mouse inner hair cell synapse: a role for Ca^{2+}-induced Ca^{2+} release. *J Physiol* **539**, 15–23.

Kim AM & Vergara JL (1998). Fast voltage gating of Ca^{2+} release in frog skeletal muscle revealed by supercharging pulses. *J Physiol* **511**, 509–518.

Koschak A, Reimer D, Huber I, Grabner M, Glossmann H, Engel J & Striessnig J (2001). alpha 1D (Cav1.3) subunits can form L-type Ca^{2+} channels activating at negative voltages. *J Biol Chem* **276**, 22100–22106.

Kros CJ & Crawford AC (1990). Potassium currents in inner hair cells isolated from the guinea-pig cochlea. *J Physiol* **421**, 263–291.

Kros CJ, Ruppersberg JP & Rusch A (1998). Expression of a potassium current in inner hair cells during development of hearing in mice. *Nature* **394**, 281–284.

Lamb GD (2000). Excitation-contraction coupling in skeletal muscle: comparisons with cardiac muscle. *Clin Exp Pharmacol Physiol* **27**, 216–224.

Langer P, Grunder S & Rusch A (2003). Expression of Ca^{2+}-activated BK channel mRNA and its splice variants in the rat cochlea. *J Comp Neurol* **455**, 198–209.

Latorre R, Vergara C & Hidalgo C (1982). Reconstitution in planar lipid bilayers of a Ca^{2+}-dependent K^+ channel from transverse tubule membranes isolated from rabbit skeletal muscle. *Proc Natl Acad Sci U S A* **79**, 805–809.

McManus OB, Helms LM, Pallanck L, Ganetzky B, Swanson R & Leonard RJ (1995). Functional role of the beta subunit of high conductance calcium-activated potassium channels. *Neuron* **14**, 645–650.

Marcotti W, Johnson SL & Kros CJ (2004). Effects of intracellular stores and extracellular Ca^{2+} on Ca^{2+}-activated K^+ currents in mature mouse inner hair cells. *J Physiol* **557**, 613–633.

Marty A (1981). Ca-dependent K channels with large unitary conductance in chromaffin cell membranes. *Nature* **291**, 497–500.

Mason MJ, Garcia-Rodriguez C & Grinstein S (1991). Coupling between intracellular Ca^{2+} stores and the Ca^{2+} permeability of the plasma membrane. Comparison of the effects of thapsigargin, 2,5-di-(tert-butyl)-1,4-hydroquinone, and cyclopiazonic acid in rat thymic lymphocytes. *J Biol Chem* **266**, 20856–20862.

Meissner G (1986). Ryanodine activation and inhibition of the Ca^{2+} release channel of sarcoplasmic reticulum. *J Biol Chem* **261**, 6300–6306.

Moser T & Beutner D (2000). Kinetics of exocytosis and endocytosis at the cochlear inner hair cell afferent synapse of the mouse. *Proc Natl Acad Sci U S A* **97**, 883–888.

Oliver D, Klocker N, Schuck J, Baukrowitz T, Ruppersberg JP & Fakler B (2000). Gating of Ca^{2+}-activated K^+ channels controls fast inhibitory synaptic transmission at auditory outer hair cells. *Neuron* **26**, 595–601.

Oliver D, Knipper M, Derst C & Fakler B (2003). Resting potential and submembrane calcium concentration of inner hair cells in the isolated mouse cochlea are set by KCNQ-type potassium channels. *J Neurosci* **23**, 2141–2149.

Pallotta BS, Magleby KL & Barrett JN (1981). Single channel recordings of Ca^{2+}-activated K^+ currents in rat muscle cell culture. *Nature* **293**, 471–474.

Platzer J, Engel J, Schrott-Fischer A, Stephan K, Bova S, Chen H, Zheng H & Striessnig J (2000). Congenital deafness and sinoatrial node dysfunction in mice lacking class D L-type Ca^{2+} channels. *Cell* **102**, 89–97.

Pyott SJ, Glowatzki E, Trimmer JS & Aldrich RW (2004). Extrasynaptic localization of inactivating calcium-activated potassium channels in mouse inner hair cells. *J Neurosci* **24**, 9469–9474.

Ransom CB, Liu X & Sontheimer H (2003). Current transients associated with BK channels in human glioma cells. *J Membr Biol* **193**, 201–213.

Raybould NP, Jagger DJ & Housley GD (2001). Positional analysis of guinea pig inner hair cell membrane conductances: implications for regulation of the membrane filter. *J Assoc Res Otolaryngol* **2**, 362–376.

Reinhart PH, Chung S, Martin BL, Brautigan DL & Levitan IB (1991). Modulation of calcium-activated potassium channels from rat brain by protein kinase A and phosphatase 2A. *J Neurosci* **11**, 1627–1635.

Roberts WM, Jacobs RA & Hudspeth AJ (1990). Colocalization of ion channels involved in frequency selectivity and synaptic transmission at presynaptic active zones of hair cells. *J Neurosci* **10**, 3664–3684.

Rudy B, Chow A, Lau D, Amarillo Y, Ozaita A, Saganich M *et al.* (1999). Contributions of Kv3 channels to neuronal excitability. *Ann N Y Acad Sci* **868**, 304–343.

Ruttiger L, Sausbier M, Zimmermann U, Winter H, Braig C, Engel J *et al.* (2004). Deletion of the Ca^{2+}-activated potassium (BK) alpha-subunit but not the BKbeta1-subunit leads to progressive hearing loss. *Proc Natl Acad Sci U S A* **101**, 12922–12927.

Samaranayake H, Saunders JC, Greene MI & Navaratnam DS (2004). Ca^{2+} and K^+ (BK) channels in chick hair cells are clustered and colocalized with apical-basal and tonotopic gradients. *J Physiol* **560**, 13–20.

Sausbier M, Hu H, Arntz C, Feil S, Kamm S, Adelsberger H *et al.* (2004). Cerebellar ataxia and Purkinje cell dysfunction caused by Ca^{2+}-activated K^+ channel deficiency. *Proc Natl Acad Sci U S A* **101**, 9474–9478.

Schopperle WM, Holmqvist MH, Zhou Y, Wang J, Wang Z, Griffith LC, Keselman I, Kusinitz F, Dagan D & Levitan IB (1998). Slob, a novel protein that interacts with the Slowpoke calcium-dependent potassium channel. *Neuron* **20**, 565–573.

Schubert R & Nelson MT (2001). Protein kinases: tuners of the BKCa channel in smooth muscle. *Trends Pharmacol Sci* **22**, 505–512.

Shi J & Cui J (2001). Intracellular Mg^{2+} enhances the function of BK-type Ca^{2+}-activated K^+ channels. *J Gen Physiol* **118**, 589–606.

Skinner LJ, Enee V, Beurg M, Jung HH, Ryan AF, Hafidi A, Aran J-M & Dulon D (2003). Contribution of BK Ca^{2+}-activated K^+ channels to auditory neurotransmission in the guinea pig cochlea. *J Neurophysiol* **90**, 320–332.

Tseng-Crank J, Foster CD, Krause JD, Mertz R, Godinot N, DiChiara TJ & Reinhart PH (1994). Cloning, expression, and distribution of functionally distinct Ca^{2+}-activated K^+ channel isoforms from human brain. *Neuron* **13**, 1315–1330.

Vergara C, Latorre R, Marrion NV & Adelman JP (1998). Calcium-activated potassium channels. *Curr Opin Neurobiol* **8**, 321–329.

Wallner M, Meera P & Toro L (1999). Molecular basis of fast inactivation in voltage and Ca^{2+}-activated K^+ channels: a transmembrane beta-subunit homolog. *Proc Natl Acad Sci U S A* **96**, 4137–4142.

Xia X, Hirschberg B, Smolik S, Forte M & Adelman JP (1998). dSLo interacting protein 1, a novel protein that interacts with large-conductance calcium-activated potassium channels. *J Neurosci* **18**, 2360–2369.

Xie J & McCobb DP (1998). Control of alternative splicing of potassium channels by stress hormones. *Science* **280**, 443–446.

Xu W & Lipscombe D (2001). Neuronal Ca(V), 1.3alpha(1), L–type channels activate at relatively hyperpolarized membrane potentials and are incompletely inhibited by dihydropyridines. *J Neurosci* **21**, 5944–5951.

Acknowledgements

We are indebted to Drs Peter Ruth and Marlies Knipper (University of Tübingen) for providing the knock-out animals of BKα and BKβ and to Drs P. Jonas and J. P. Adelman for reading the manuscript. This work was supported by a grant from the Deutsche Forschungsgemeinschaft to B.F. (Fa 332/5-1) and the Graduiertenkolleg GRK 843.